

## **Electronic Supplementary Information**

*Journal of Materials Chemistry C*

# **Open system synthesis of narrow-bandwidth red-fluorescent carbon quantum dots with a function of multi-metal ion sensing**

Rika Katakami, Kohei Sato, Akihiro Ogura, Ken-ichi Takao, Yoshiki Iso,<sup>\*</sup> and Tetsuhiko Isobe<sup>\*</sup>

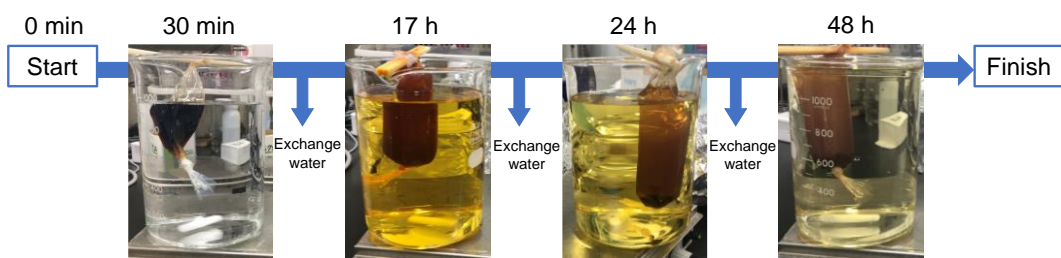
*Department of Applied Chemistry, Faculty of Science and Technology, Keio University,  
3-14-1 Hiyoshi, Kohoku-ku, Yokohama 223-8522, Japan*

<sup>\*</sup>Corresponding authors.

Yoshiki Iso – E-mail: iso@aplc.keio.ac.jp; Tel.: +81 45 566 1558; Fax: +81 45 566 1551; orcid.org/0000-0001-7483-2828

Tetsuhiko Isobe – E-mail: isobe@aplc.keio.ac.jp; Tel.: +81 45 566 1554; Fax: +81 45 566 1551; orcid.org/0000-0002-0868-5425

### PG-CQDs



### DAR-CQDs

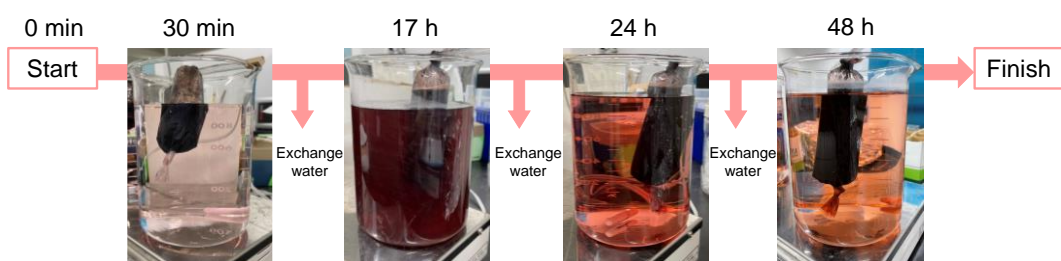


**Fig. S1.** Purification of PG-CQDs and DAR-CQDs by dialysis.

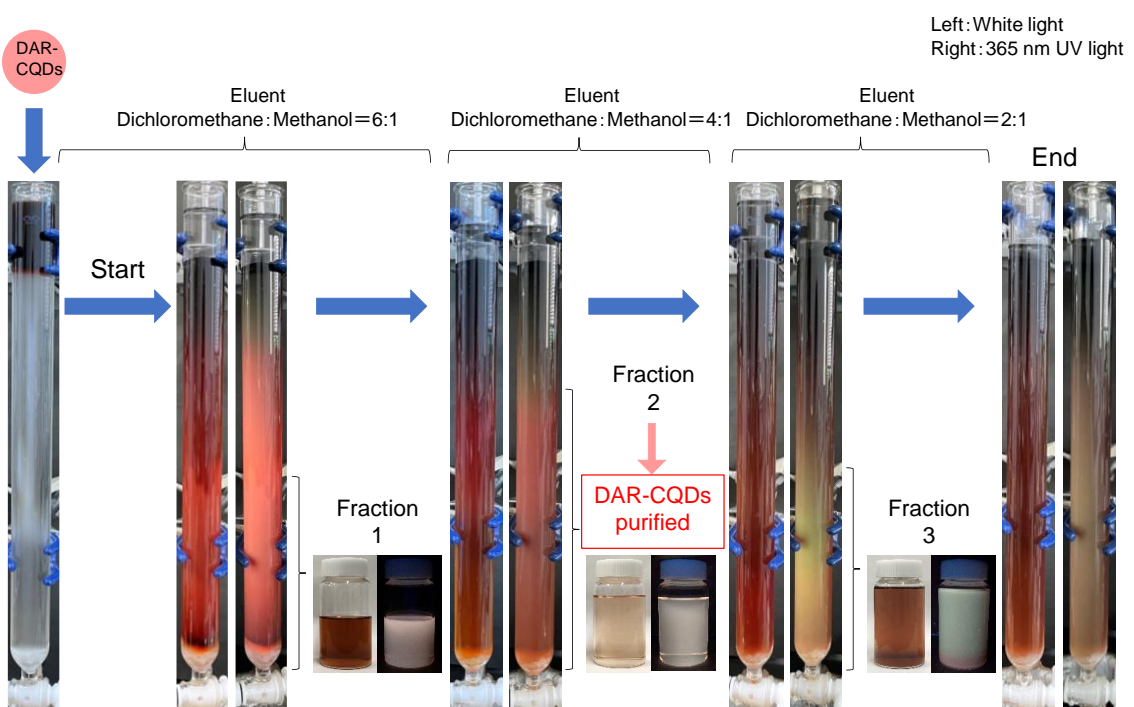
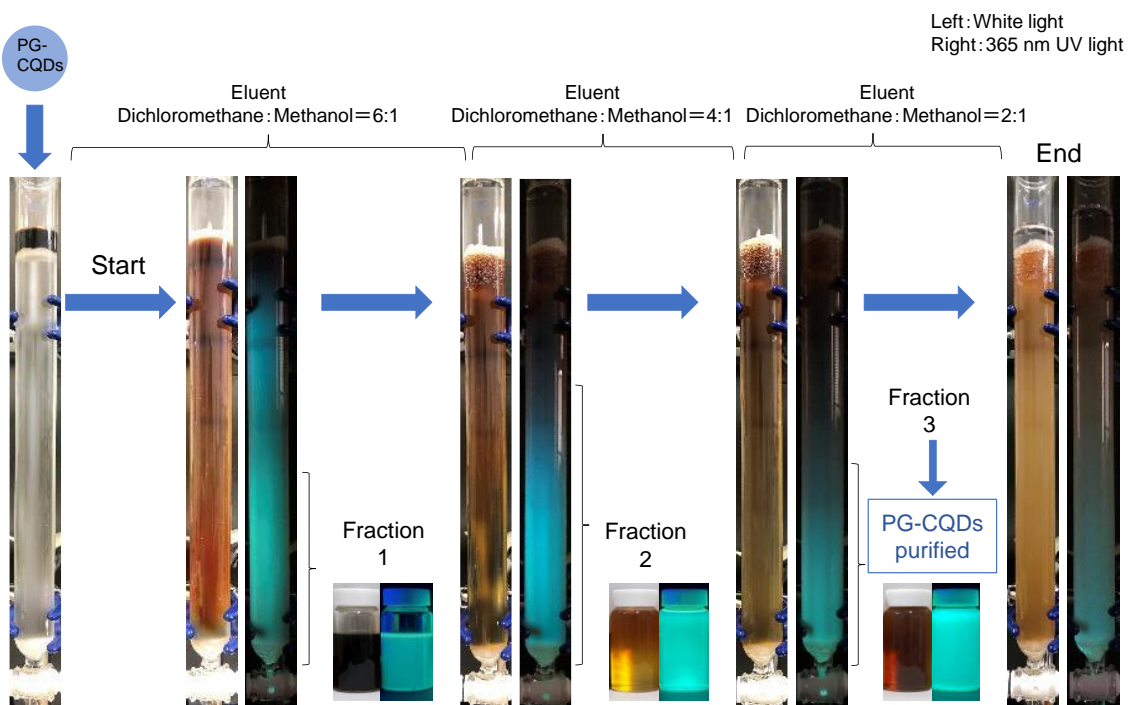


**Fig. S2.** Purification of PG-CQDs and DAR-CQDs by silica gel column chromatography.

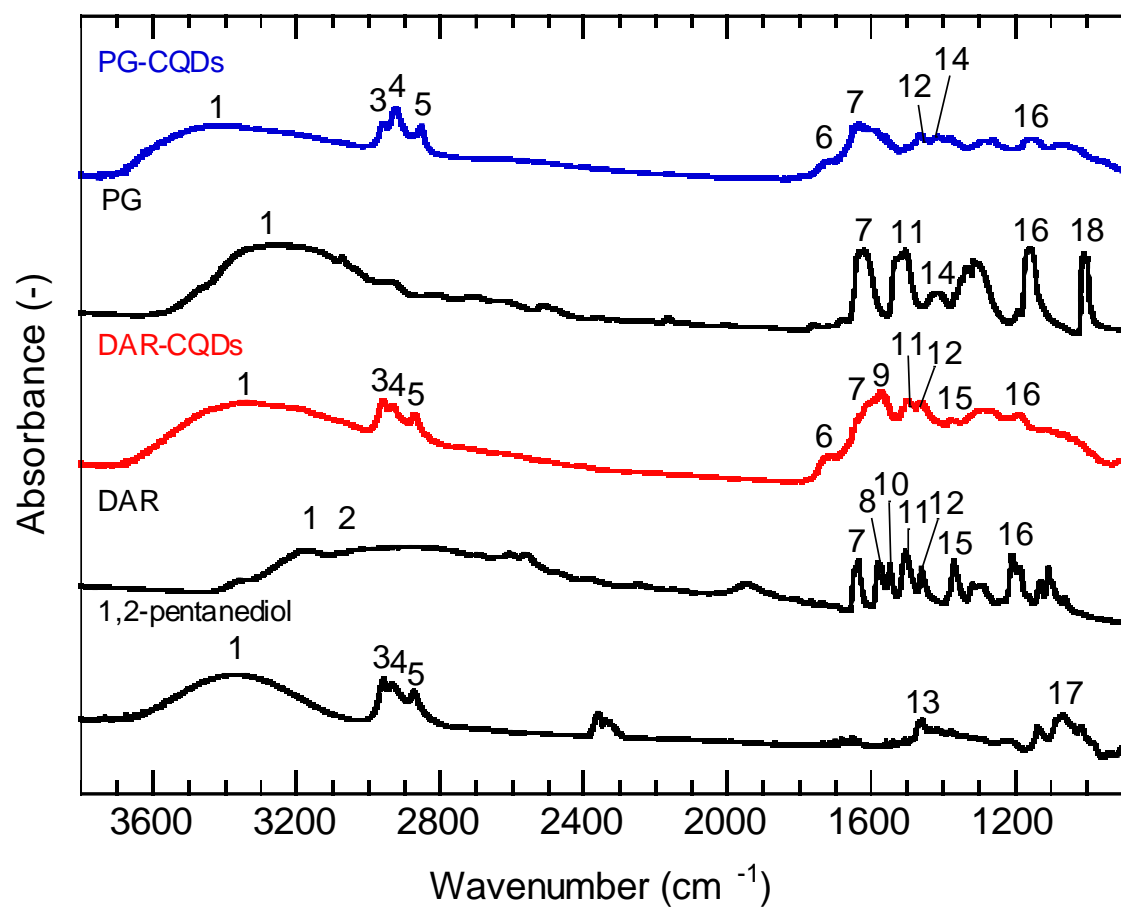


**Fig. S3.** FT-IR spectra of PG-CQDs, PG, DAR-CQDs, DAR, and 1,2-pentanediol.

**Table S1.** Assignments of FT-IR absorption peaks of Fig. S3.

Peak	Wavelength (cm <sup>-1</sup> )				Assignment
	PG-CQDs	PG	DAR-CQDs	DAR	
1			3100–3600		v(O–H)
2			3100–3600		v(NH <sub>2</sub> )
3	2958		2959		v <sub>as</sub> (CH <sub>3</sub> )
4	2925		2933		v <sub>s</sub> (CH <sub>3</sub> )
5	2872		2873		v <sub>s</sub> (CH <sub>2</sub> )
6	1713		1713		v(C=O)
7	1651	1622	1652	1636	ring(C=C)
8				1580	δ <sub>as</sub> (NH <sub>3</sub> <sup>+</sup> )
9			1570		δ(NH <sub>2</sub> )
10				1548	δ <sub>s</sub> (NH <sub>3</sub> <sup>+</sup> )
11		1506			ring semicircle stretching
12	1467		1468	1460	ring semicircle stretching
13				1457	δ(CH <sub>2</sub> )
14	1415	1418			δ(O–H)
15			1378	1370	v(C–N)
16	1160	1158	1190	1207	v(C–O)
17				1067	v <sub>as</sub> (C–C–O)
18		1008			δ(C–H)

v=stretching, δ=deformation or bending, as=asymmetric, s=symmetric

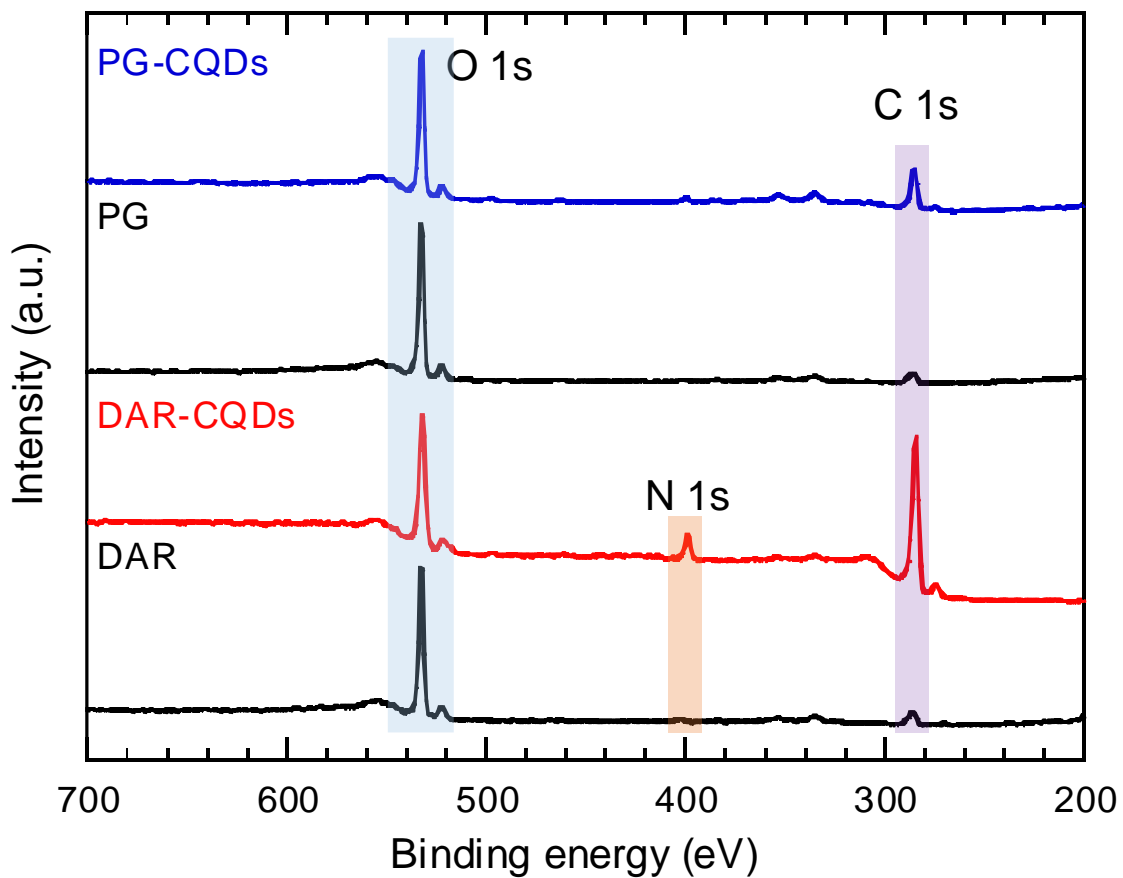


**Fig. S4.** XPS survey spectra of PG-CQDs, PG, DAR-CQDs, and DAR.

**Table S2.** Proportions of different bonds calculated from peak fitting of the C (1s) XPS spectra of PG, PG-CQDs, DAR, and DAR-CQDs.

Sample	C–OH [%]	C=C/C–C/C–N [%]
PG (Calculated)	50	50
PG (Measured)	45.9	54.1
PG-CQDs (Measured)	19.3	80.7
DAR (Calculated)	33.3	66.6
DAR (Measured)	27.3	72.7
DAR-CQDs (Measured)	1.5	89.5

Calculated: obtained from molecular structure.

Measured: obtained from peak fitting of C (1s) XPS spectrum.

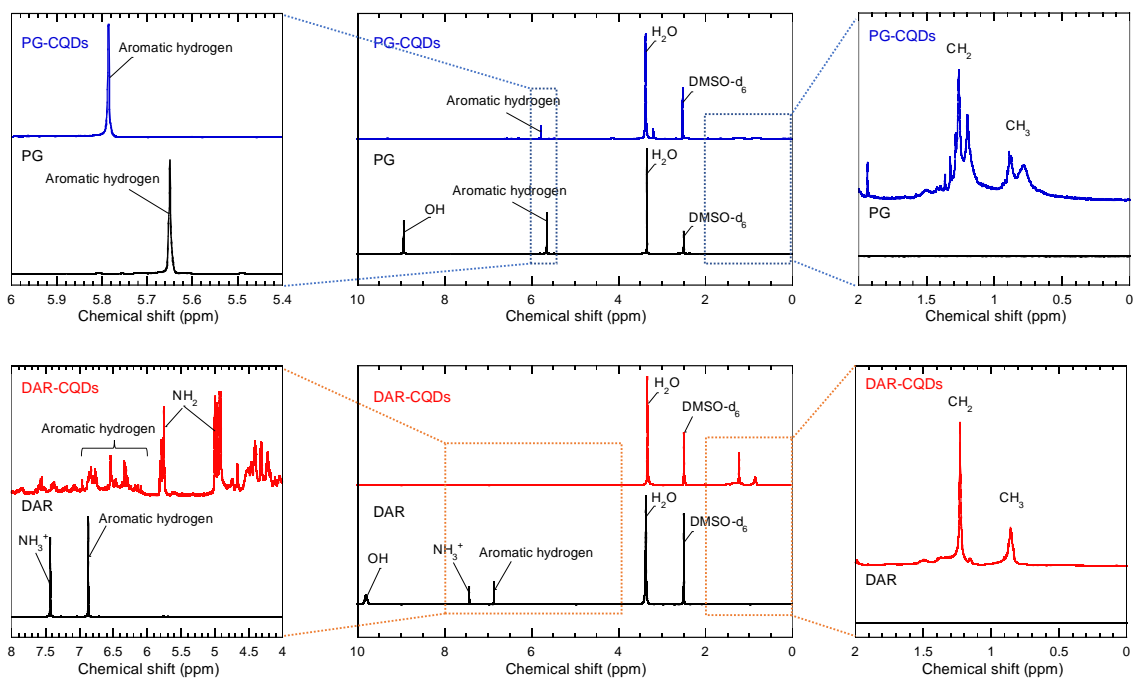


**Fig. S5.**  $^1\text{H}$ -NMR spectra of PG-CQDs and DAR-CQDs.

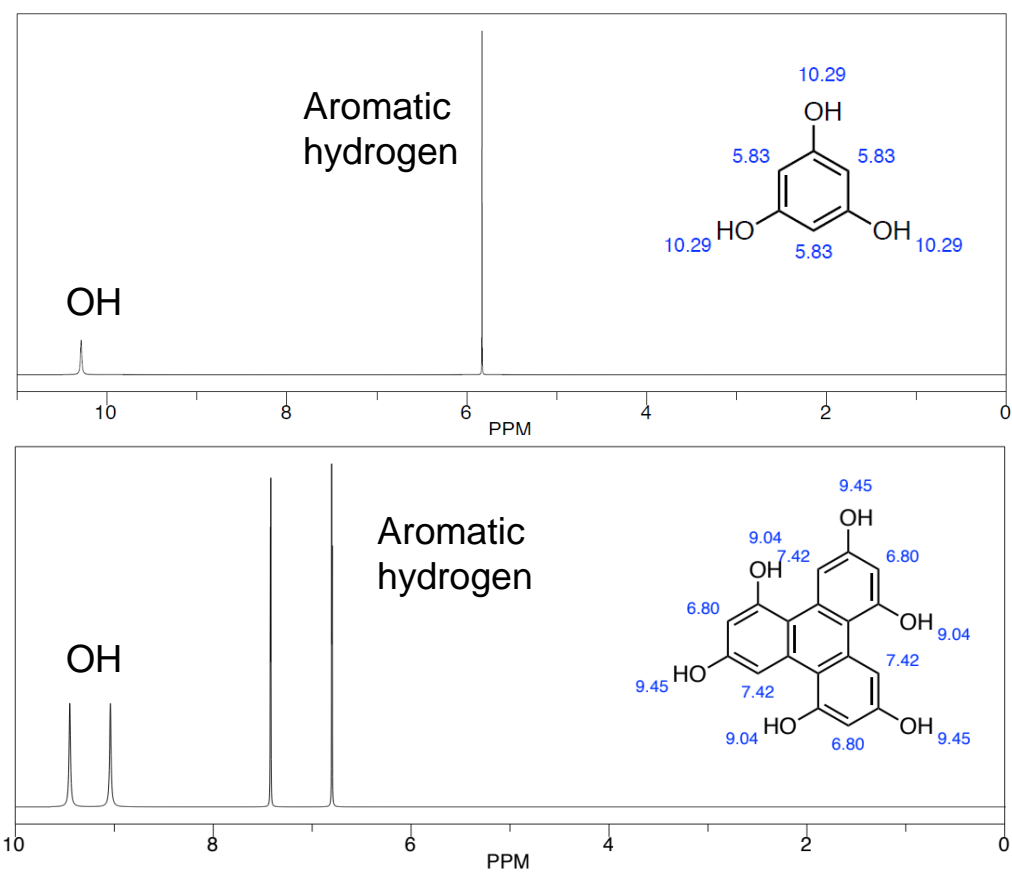


**Fig. S6.** Simulated <sup>1</sup>H-NMR spectra of PG and the molecule formed by dehydration condensation of three PG molecules.

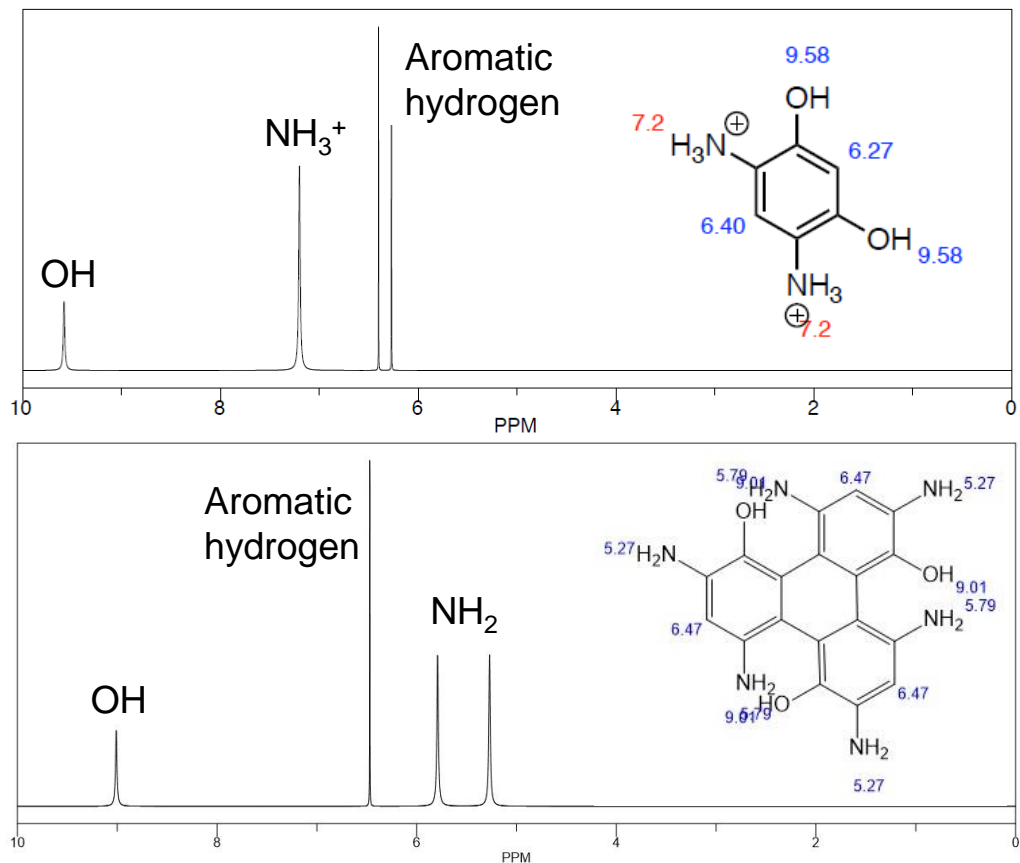


**Fig. S7.** Simulated  $^1\text{H}$ -NMR spectra of DAR and the molecule formed by dehydration condensation of three DAR molecules.

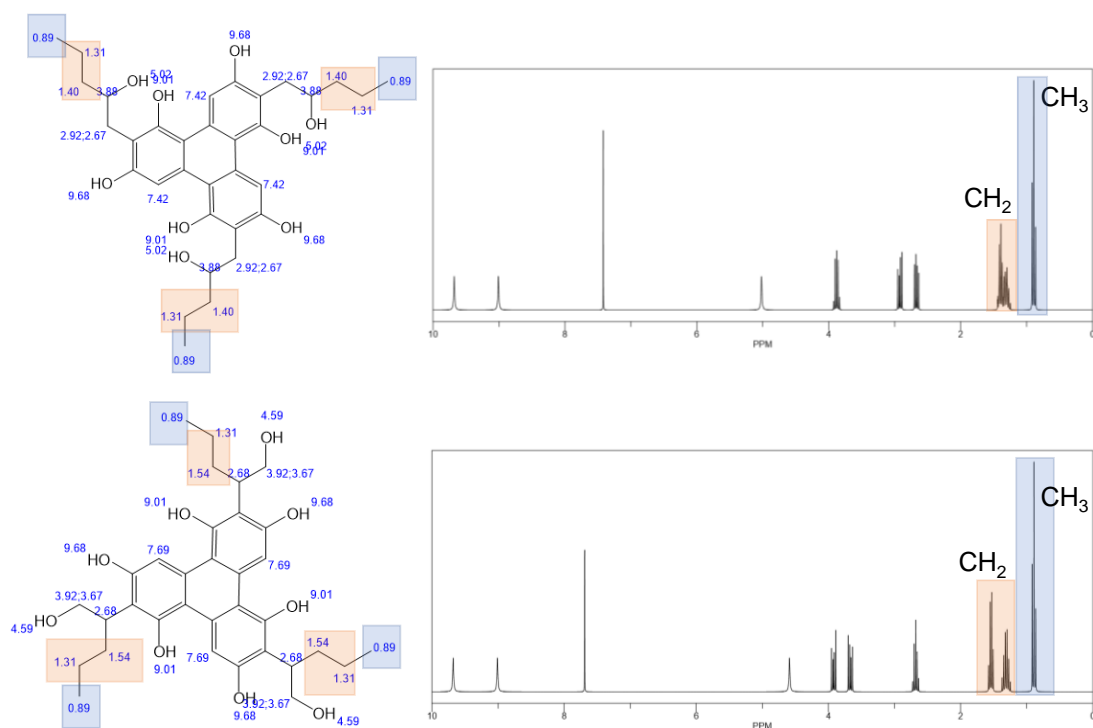


**Fig. S8.** Simulated  $^1\text{H}$ -NMR spectra of the dehydration-condensed structure of three PG molecules bonded to three 1,2-pentanediol molecules.

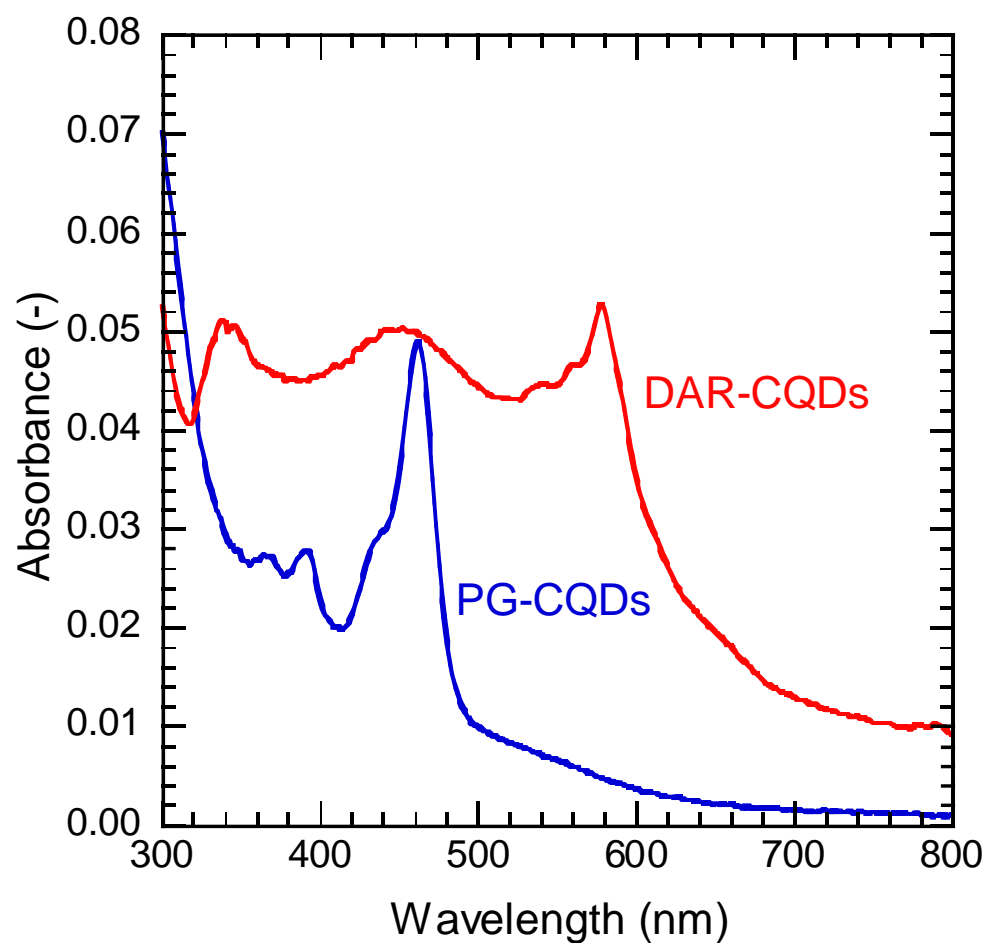


**Fig. S9.** UV-vis spectra of ethanol dispersions of PG-CQDs and DAR-CQDs.

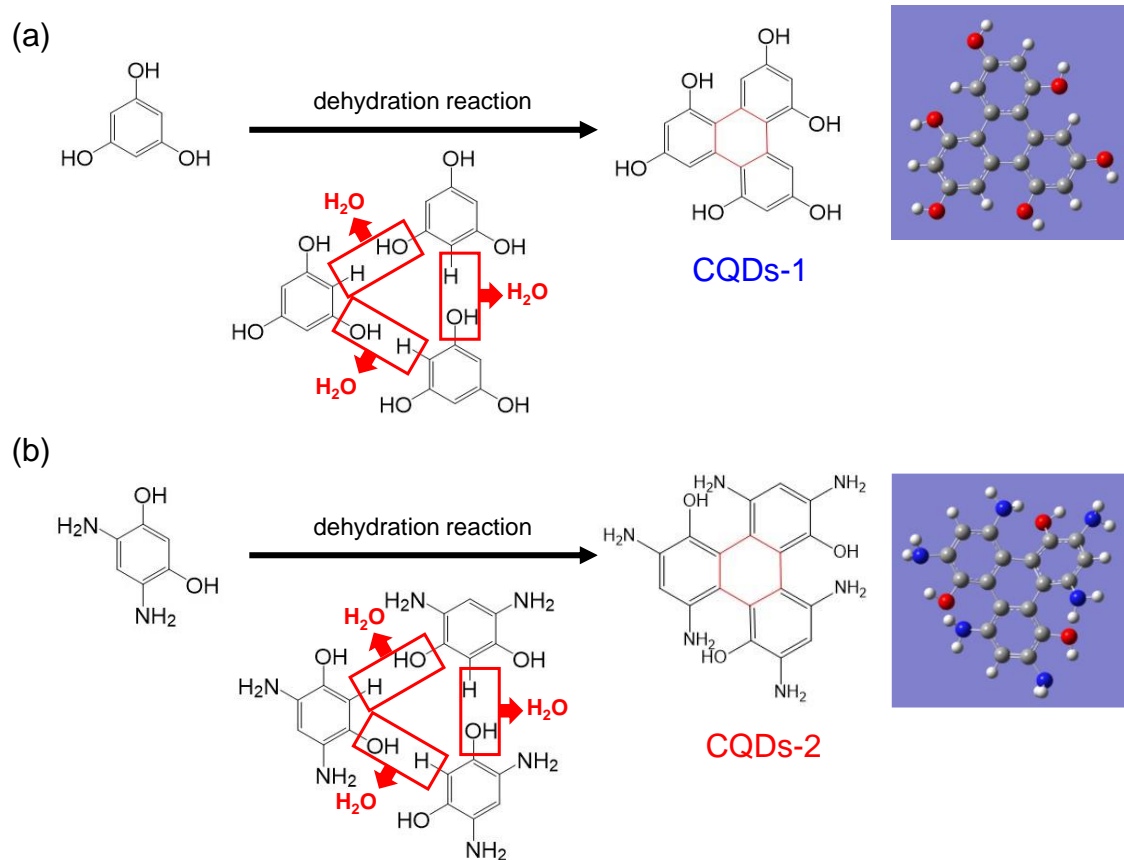


**Fig. S10.** Structural models and optimized structures of CQDs-1 and CQDs-2.

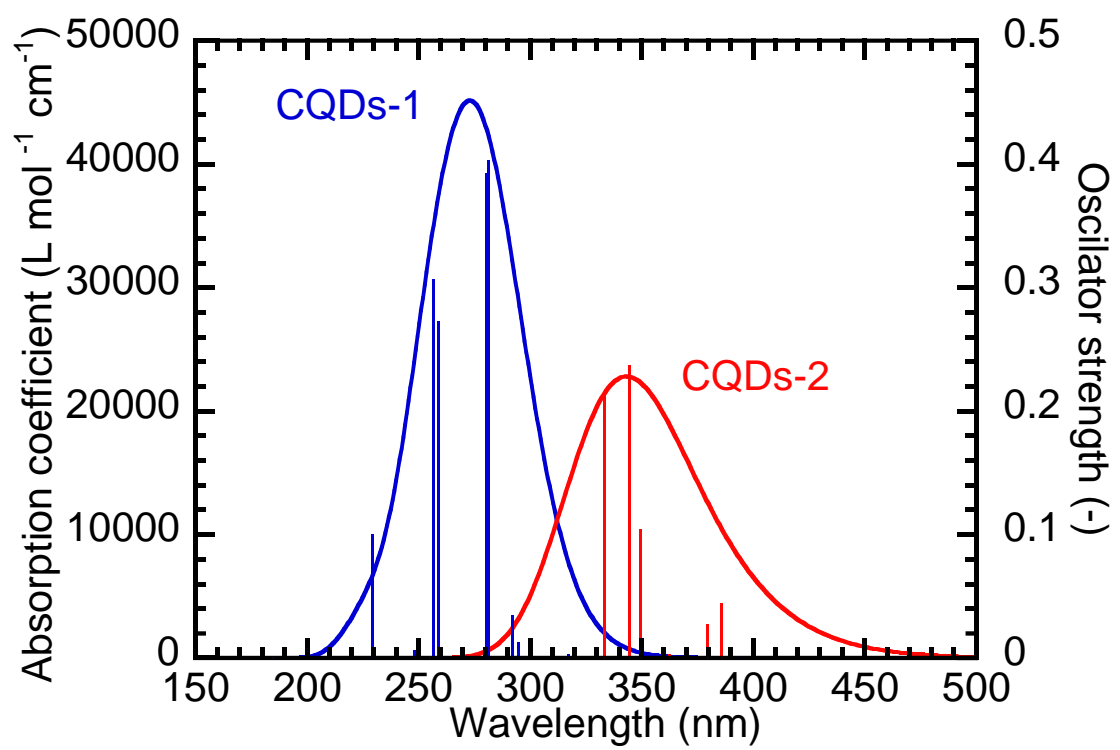


**Fig. S11.** UV-vis absorption spectra with oscillator strength (vertical lines) of CQDs-1 and CQDs-2 obtained by TD-DFT calculations.

**Table S3.** HOMO/LUMO energy levels and HOMO-LUMO energy gaps  $E_{\text{H-L}}$  of CQDs-1, CQDs-2, and CQDs-3.

Sample	HOMO (eV)	LUMO (eV)	$E_{\text{H-L}}$ (eV)	$E_{\text{H-L}}$ (nm)
CQDs-1	-5.044	-0.487	4.557	272
CQDs-2	-4.349	-0.543	3.806	326
CQDs-3	-4.352	-0.890	3.462	358

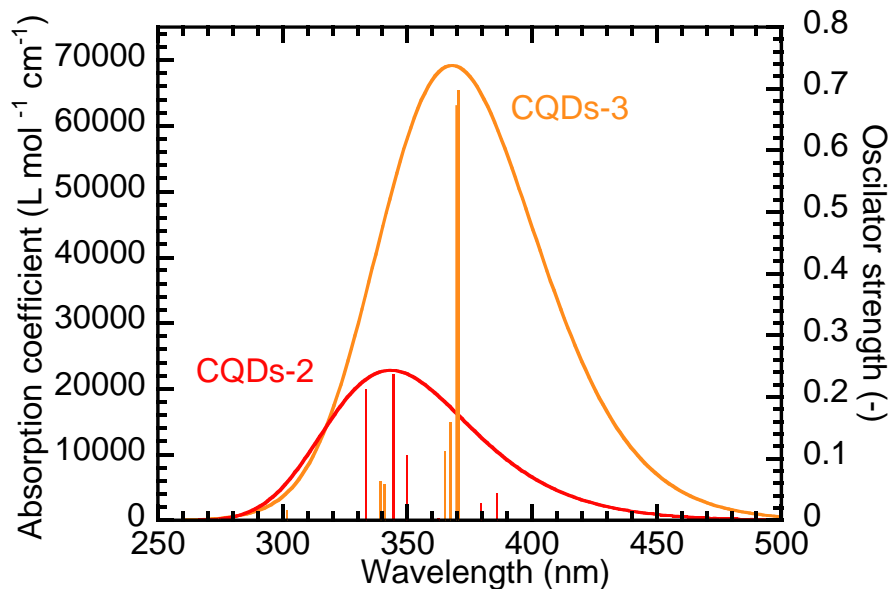
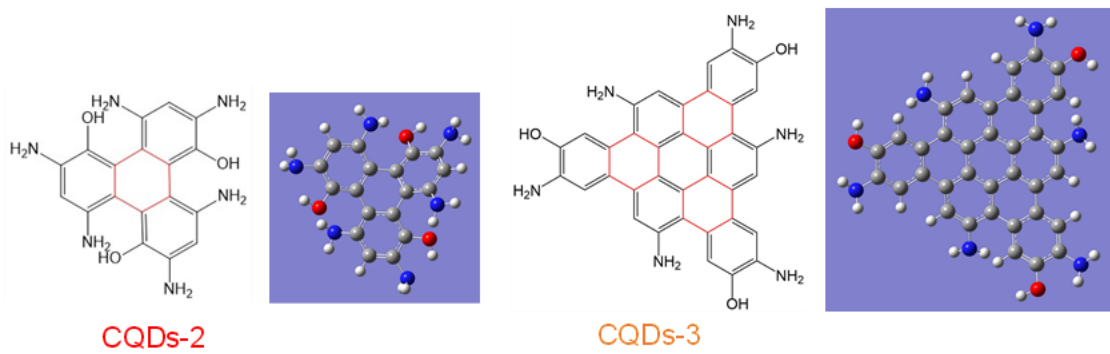


**Fig. S12.** Structural models and optimized structures of CQDs-2 and CQDs-3, and their UV-vis absorption spectra with oscillator strength (vertical lines) obtained by TD-DFT calculations.

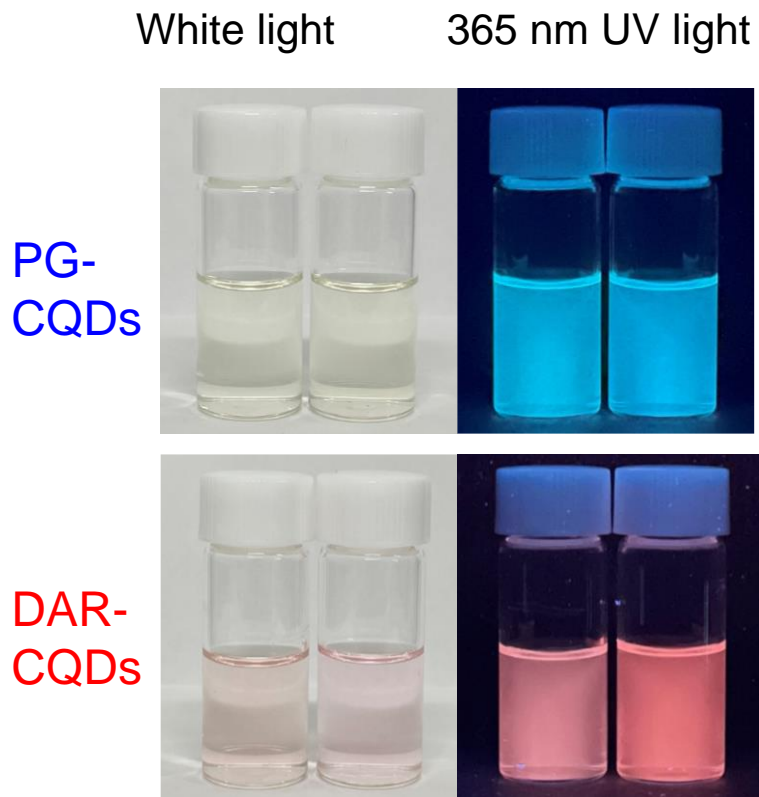


**Fig. S13.** Photographs of PG-CQDs and DAR-CQDs dispersions in methanol (left) and deuterated methanol (right).

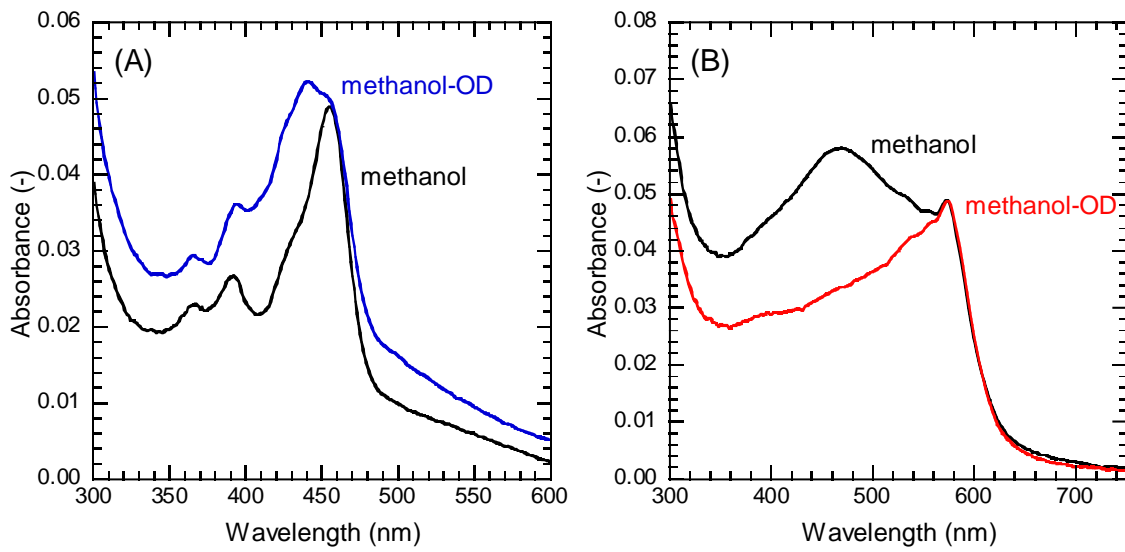


**Fig. S14.** UV-vis spectra of (A) PG-CQDs and (B) DAR-CQDs dispersions in methanol and deuterated methanol.

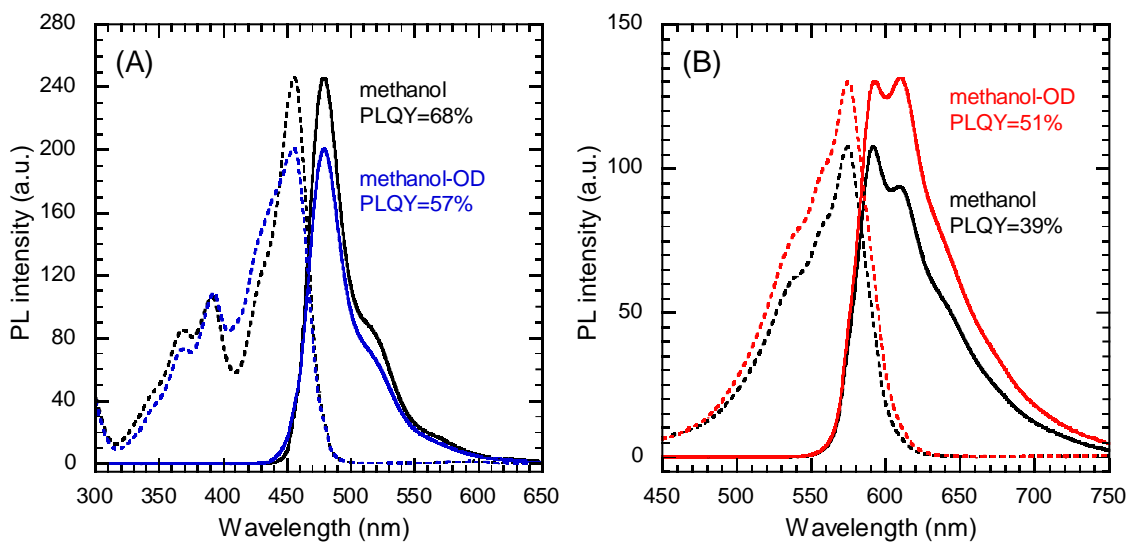


**Fig. S15.** PLE and PL spectra of (A) PG-CQDs and (B) DAR-CQDs dispersions in methanol and deuterated methanol.

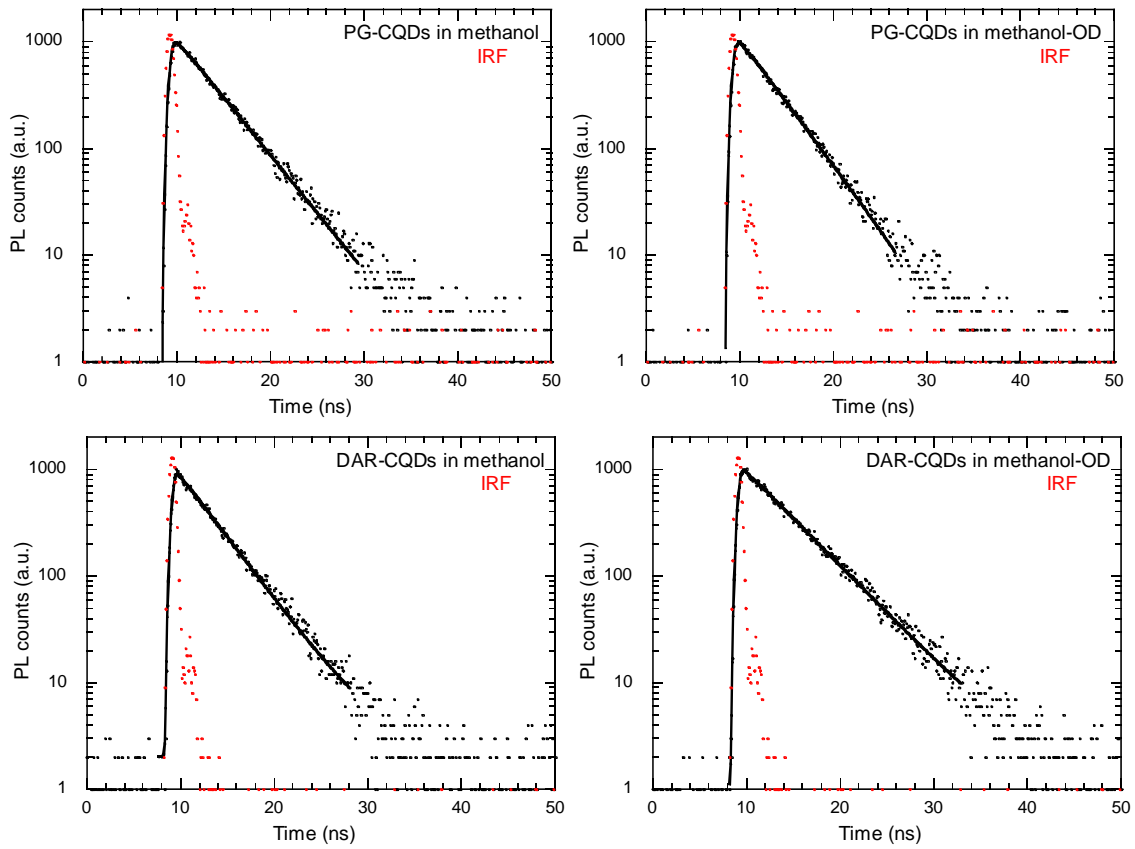


**Fig. S16.** PL decay curves of PG-CQDs and DAR-CQDs dispersions in methanol and deuterated methanol.  $\lambda_{\text{ex}}$ : PG-CQDs 405 nm, DAR-CQDs 590 nm.

**Table S4.** PLQYs of PG-CQD and DAR-CQD ethanol dispersions before and after storage for 26 months in the dark at room temperature.

Sample	Storage duration (month)	PLQY
PG-CQDs	0	56
	26	53
DAR-CQDs	0	30
	26	32

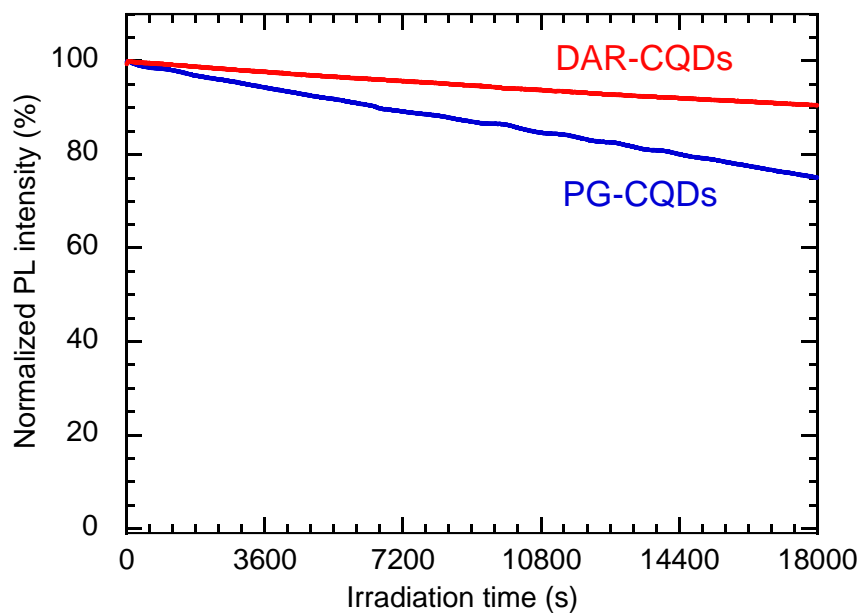


**Fig. S17.** Changes in PL intensities of PG-CQD and DAR-CQD ethanol dispersions with the irradiation time measured under each optimum excitation wavelength.

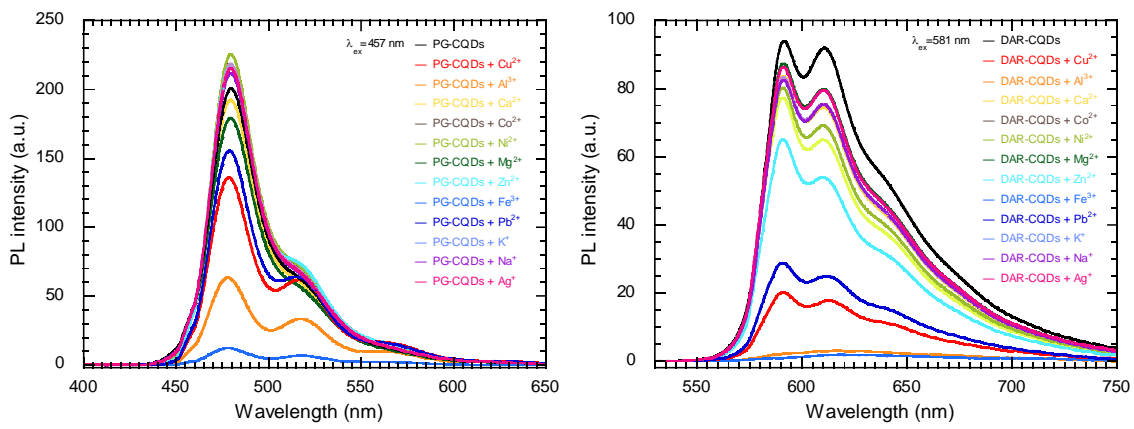


**Fig. S18.** The PL spectra of PG-CQDs and DAR-CQDs aqueous dispersions in the

absence and presence of different metal ions.